

**Original citation:**

Hou, Lei, Sun, Baojiang, Geng, Xueyu , Jiang, Tingxue and Wang, Zhiyuan. (2016) Study of the slippage of particle / supercritical CO<sub>2</sub> two-phase flow. Journal of Supercritical Fluids.

**Permanent WRAP URL:**

<http://wrap.warwick.ac.uk/82084>

**Copyright and reuse:**

The Warwick Research Archive Portal (WRAP) makes this work by researchers of the University of Warwick available open access under the following conditions. Copyright © and all moral rights to the version of the paper presented here belong to the individual author(s) and/or other copyright owners. To the extent reasonable and practicable the material made available in WRAP has been checked for eligibility before being made available.

Copies of full items can be used for personal research or study, educational, or not-for-profit purposes without prior permission or charge. Provided that the authors, title and full bibliographic details are credited, a hyperlink and/or URL is given for the original metadata page and the content is not changed in any way.

**Publisher's statement:**

© 2016, Elsevier. Licensed under the Creative Commons Attribution-NonCommercial-NoDerivatives 4.0 International <http://creativecommons.org/licenses/by-nc-nd/4.0/>

**A note on versions:**

The version presented here may differ from the published version or, version of record, if you wish to cite this item you are advised to consult the publisher's version. Please see the 'permanent WRAP URL' above for details on accessing the published version and note that access may require a subscription.

For more information, please contact the WRAP Team at: [wrap@warwick.ac.uk](mailto:wrap@warwick.ac.uk)

# Study of the slippage of particle / supercritical CO<sub>2</sub> two-phase flow

Lei Hou <sup>a,b</sup>, Baojiang Sun <sup>a\*</sup>, Xueyu Geng <sup>c</sup>, Tingxue Jiang <sup>b</sup>, Zhiyuan Wang <sup>a</sup>

<sup>a</sup> School of Petroleum Engineering, China University of Petroleum (East China), 66 Changjiang West Rd, Qingdao 266580, China

<sup>b</sup> SINOPEC Research Institute of Petroleum Engineering, Beijing 100101, China

<sup>c</sup> School of Engineering, The University of Warwick, Coventry, UK, CV4 7AL

**Abstract** In this paper, the slippage velocity and displacement between particles and supercritical CO<sub>2</sub> (SC-CO<sub>2</sub>) were studied to reveal the particle-SC-CO<sub>2</sub> two-phase flow behavior. Visualization experiments were performed to directly measure the slippage velocity and displacement. Eight groups of experiments involving various pressures (7.89–10.96 MPa), temperatures (38.6–47.5 °C), particle diameters (0.3–0.85 mm), particle densities (2630 and 3120 kg/m<sup>3</sup>) and SC-CO<sub>2</sub> flow rates (0.920–1.284 m/s) were conducted. The measured particle slippage velocities in the flowing direction were approximately 10.3 % of the SC-CO<sub>2</sub> flow rate. The measured particle slippage displacements were all at the centimeter level, which indicated that SC-CO<sub>2</sub> had a superior particle transporting capability that was similar to those of liquids even if it had a low viscosity that was similar to those of gases. A numerical model was built, and analytic slippage calculations were performed for SC-CO<sub>2</sub> for additional analyses. The density of SC-CO<sub>2</sub> was found to have a greater influence on the slippage than the viscosity. Moreover, a comparison of the slippage between SC-CO<sub>2</sub> and water showed that the particle slippage in water was constant, while the particle slippage in SC-CO<sub>2</sub> continually accumulated at an extremely slow rate.

**Keywords:** supercritical CO<sub>2</sub>; two-phase flow; visualization experiments; analytic calculations; slippage behavior

\* Corresponding author. Tel.: +86 532 86983137; fax: +86 532 86983137  
E-mail address: sunbj1128@126.com (Baojiang Sun)

## 1. Introduction

Supercritical CO<sub>2</sub> (SC-CO<sub>2</sub>), which has recently been introduced to petroleum engineering, can be used as a drilling or fracturing fluid and is an efficient and environmentally friendly petroleum engineering fluid. Basic research has been conducted on SC-CO<sub>2</sub> applications in drilling and fracturing processes in recent years [1–4]. Street et al. [5] and Khanpour et al. [6] treated drilling fluid waste using SC-CO<sub>2</sub> and obtained efficient results. Du et al. [7,8] developed a large-scale SC-CO<sub>2</sub> circulating platform and performed SC-CO<sub>2</sub> jet experiments. The results showed higher efficiency with the SC-CO<sub>2</sub> jet than with the water jet. Sun et al. [9] and Wu et al. [10] used experimental and numerical methods to study the adsorption-desorption properties of supercritical CO<sub>2</sub> in shale. Wang et al. [11,12] performed a friction coefficient calculation of SC-CO<sub>2</sub> pipe flow and improved the SC-CO<sub>2</sub> density calculation method.

All of the previous studies described above have mainly focused on single-phase SC-CO<sub>2</sub>. However, solid phase (drilling cut or proppant) transport is one of the essential uses of fluids in petroleum engineering [13,14]. It is SC-CO<sub>2</sub> multi-phase flow rather than single-phase flow that occurs in most field applications. For instance, one of the primary tasks of SC-CO<sub>2</sub> as a fracturing fluid is carrying the proppant (fine ceramics or sand) as deeply as possible into the fracture in the horizontal direction.

The low-viscosity and high-density features of SC-CO<sub>2</sub> shroud its transporting capability. Particles transported in gases, which have low viscosities compared to SC-CO<sub>2</sub>, have more serious slippage than particles transported in liquids, which have high densities compared to SC-CO<sub>2</sub>. It is unclear whether SC-CO<sub>2</sub> has a low transporting capability similar to gases, a superior capability similar to liquids, or a capability that is between those of gases and liquids. Hence, solid phase transport has

1 become one of the technique bottlenecks when using SC-CO<sub>2</sub>, and more studies on SC-CO<sub>2</sub>  
2  
3 multi-phase flow are needed.  
4

5  
6 However, SC-CO<sub>2</sub> multi-phase flow research has rarely been conducted, even in supercritical  
7  
8 fluids research where studies have mainly focused on chemical properties. Therefore, this paper  
9  
10 examines SC-CO<sub>2</sub> and particle two-phase flow. Experiments were performed to directly measure  
11  
12 the slippage velocity and displacement. The features of particle slippage in SC-CO<sub>2</sub> were analyzed  
13  
14 by using a numerical model, and analytic calculations were derived. The results can be applied for  
15  
16 the particle-SC-CO<sub>2</sub> two-phase flow analysis in particle tracing, fluidization, transportation, etc.  
17  
18  
19  
20  
21

## 22 **2. Materials and methods**

### 23 **2.1 Materials**

24  
25 Ceramic particles, which are widely used in the petroleum industry as proppant for fracturing,  
26  
27 were chosen for their uniform density and sphericity. Two different densities (2630 kg/m<sup>3</sup> and  
28  
29 3120 kg/m<sup>3</sup>) and meshes (0.3~0.85 mm in diameter) of particles were used. The ceramic particles  
30  
31 were obtained from Down-hole Service Co. at the Shengli Oil Field (SINOPEC). CO<sub>2</sub> with a  
32  
33 purity of 99.99 % was purchased from Tianyuan Gas Product Co. (Qingdao, China).  
34  
35  
36  
37  
38  
39  
40  
41

### 42 **2.2 Apparatus and procedures**

43  
44 Experiments on particle motion following with supercritical CO<sub>2</sub> were conducted in a  
45  
46 visualization apparatus. More detailed descriptions of the apparatus, the operating procedures  
47  
48 and the data processes can be found in Hou et al. [15]. The experimental setup consists of an  
49  
50 SC-CO<sub>2</sub> supply system and a visualization module. The CO<sub>2</sub> is heated by a water bath to the  
51  
52 supercritical state. The transient flow rate is recorded by an electromagnetic flowmeter group [8].  
53  
54  
55  
56  
57  
58 The visualization module is composed of a visualization channel simulator and a high-speed  
59  
60  
61  
62  
63  
64  
65

1 camera system, as shown in Figure 1. The channel simulator consists of four identical units,  
2  
3 which can be freely disassembled and combined. The simulated channel has a fixed width of 5  
4  
5 mm, a height of 50 mm and a length of 250 mm for each unit. Each unit has two pairs of  
6  
7 observation windows, as shown in Figure 1, through which the particle movements are filmed.  
8  
9 The maximum working pressure of the visualization module is 30 MPa. The high-speed camera  
10  
11 is an OLYMPUS I-speed TR, which has a maximum resolution of  $1280 \times 1024$  at a speed of  
12  
13 2000 fps. The light source (SHIBUYA JHP-40WP) is an LED cold-light illuminator, which does  
14  
15 not affect the temperature of the SC-CO<sub>2</sub> in the stimulated channel.  
16  
17  
18  
19  
20  
21

22 During the experimental process, the high-speed camera system was placed on both sides of the  
23  
24 second window from the SC-CO<sub>2</sub> inlet. A small amount of particles was mixed in from the inlet  
25  
26 above the first window (from the SC-CO<sub>2</sub> inlet). The particle motion was recorded by the camera,  
27  
28 and, simultaneously, the temperature, pressure and flow rate were all noted. Thus, each record of  
29  
30 the particle motion has corresponding temperature, pressure and flow rate notes.  
31  
32  
33  
34  
35

36 The experimental data were processed using the OLYMPUS I-speed control software. The  
37  
38 diameter, horizontal velocity and displacement of the particle in each time unit were obtained  
39  
40 using picture-by-picture analysis. The average uncertainty of the experimental apparatus and the  
41  
42 method is 0.19 % [15].  
43  
44  
45  
46

### 47 **2.3 Particle horizontal motion model**

48 Numerical analyses were also applied to reveal the characteristics of the SC-CO<sub>2</sub> and particle  
49  
50 two-phase flow. The particle motion model was built based on the Basset-Boussinesq-Oseen  
51  
52 (BBO) equation [16]. Considering that the effects of flowing friction, wall effects and roughness  
53  
54  
55  
56  
57  
58  
59  
60  
61  
62  
63  
64  
65

on the particle-SC-CO<sub>2</sub> two-phase flow are still unclear, the particle horizontal motion model was built based on the following assumptions:

- (1) The SC-CO<sub>2</sub> flow is a steady, uniform flow;
- (2) The particle/particle and particle/wall interactions are ignored.

By analyzing the forces (drag force, virtual mass force and Basset force) acting on a single particle in the flowing SC-CO<sub>2</sub>, the particle horizontal motion differential equation is

$$\frac{\pi d_p^3}{6} \rho_p \frac{dv_p}{dt} = \frac{\pi d_p^2}{8} \rho_f (v_f - v_p)^2 C_D - \frac{\pi d_p^3}{12} \rho_f \frac{dv_p}{dt} - \frac{3d_p^2}{2} (\pi \rho_f \mu)^{1/2} \int_0^t \frac{dv_p}{\sqrt{t-\tau}} d\tau \quad (1)$$

where  $d_p$  is the diameter of the particle,  $\rho_p$  is the density of the particle,  $v_p$  is the horizontal velocity of the particle,  $\rho_f$  is the SC-CO<sub>2</sub> density,  $v_f$  is the SC-CO<sub>2</sub> flow rate,  $C_D$  is the drag coefficient,  $\mu$  is the SC-CO<sub>2</sub> viscosity,  $t$  is the time, and  $\tau$  is the relaxation time.

The drag coefficient ( $C_D$ ) is the key parameter in the drag force expression. However, there are no relevant reports on the specific drag coefficient calculation in SC-CO<sub>2</sub>. Hence, an auxiliary equation set is established based on the power-law settling velocity calculation [15] to solve the drag coefficient indirectly. The equation set is

$$\begin{cases} C_D = \frac{4g(\rho_p - \rho_f)d_p}{3v_\infty^2 \rho_f} \\ v_\infty = \frac{\mu}{\rho_f d_p} [0.1196 \left(\frac{\rho_p}{\rho_f}\right)^2 - 0.1216 \frac{\rho_p}{\rho_f} - 0.2961] Ar^{[-0.214 \ln(\frac{\rho_p}{\rho_f}) + 0.8241]} \\ Ar = \frac{g(\rho_p - \rho_f) \rho_f d_p^3}{\mu^2} \end{cases} \quad (2)$$

where  $v_\infty$  is the terminal settling velocity of particles in SC-CO<sub>2</sub>,  $g$  is the acceleration due to gravity, and  $Ar$  is the particle Archimedes number.

The Basset force, which is also called the history force, is caused by the relative acceleration between the particles and the SC-CO<sub>2</sub>. The Basset force expression in Eq. (1) is an integration and could be solved using the methods of Shenhua et al. [17] and Bombardelli et al. [18], who proved the convergence of the Basset force expression. The fractional integral method can be used to eliminate the integral singularity. The trapezoid formula can then be applied to discretize the integral term. The approximation of the integral term is given by

$$\int_0^t \frac{dv_p}{\sqrt{t-\tau}} d\tau \approx \frac{h}{2} \left( \frac{a_0}{\sqrt{i \cdot h}} + 2 \sum_{j=2}^{i-2} \frac{a_j}{\sqrt{i \cdot h - j \cdot h}} + \frac{a_{i-1}}{\sqrt{h}} \right) + (a_i + a_{i-1}) \sqrt{h} \quad (3)$$

where  $h$  is the time unit,  $a_0$  is the initial ( $t=0$ ) particle acceleration, and  $a_i$  is the particle horizontal acceleration at moment  $t_i$ .

Combining Eqs. (1), (2) and (3), the governing equation for the particle horizontal motion model can be given. In this model, the drag coefficient ( $C_D$ ) is calculated by a new indirect method. The new method is based on the SC-CO<sub>2</sub> experiment [15] and is therefore more suitable for the SC-CO<sub>2</sub> case than other methods based on conventional fluid experiments.

The particle horizontal motion model is discretized using the Euler method and solved by programming in VB.NET.

### 3 Results and discussion

#### 3.1 Experimental results

Eight groups of experiments were conducted under various temperature, pressure and particle conditions, as shown in Table 1. In each group of experiments, at least ten particles were selected randomly and processed to obtain a set of horizontal velocities and displacements. For a single particle, the motion can be affected by particle shape, roughness, wall effects, etc., which may

1 induce strong randomness in its velocity and displacement. Therefore, the average values of the  
2  
3 particle velocity and displacement are presented in Table 1.  
4

5  
6 The average particle velocities in the flow direction fall in the range of 0.843–1.204 m/s, which  
7  
8 reach an average of 89.7 % of the SC-CO<sub>2</sub> flow velocity. The average slippage displacements fall  
9  
10 in the range of 0.0135–0.0341 m and are all at the centimeter level. The directly measured  
11  
12 slippage velocities and displacements between the particles and the SC-CO<sub>2</sub> were relatively small.  
13  
14  
15  
16  
17 Based on experimental measurements, SC-CO<sub>2</sub> was found to have a superior particle transporting  
18  
19 capability that was similar to a liquid even if it had a low viscosity that was similar to that of a gas.  
20  
21

### 22 **3.2 Verification of the particle horizontal motion model**

23

24  
25 The experimental results are used to verify the particle motion model. During the experiments,  
26  
27 the frame rate of the camera was set to 1/4000 s. The directly measured parameters were the  
28  
29 particle horizontal velocity and displacement in each time unit, which was 1/4000 s. The particle  
30  
31 inlet (as shown in Fig. 1) was selected as the origin. Based on the relative position between the  
32  
33 particle inlet and the observation windows, the center coordinate of the second window is known.  
34  
35  
36  
37 According to the coordinates of the window center, the particle horizontal displacement ( $L_1$ )  
38  
39 from the inlet can be measured at the time when it enters the observation window. Similarly, the  
40  
41 displacement ( $L_2$ ) can be obtained at the moment when the particle moves out of the window.  
42  
43  
44  
45 During this displacement, the particle horizontal velocity and displacement in each time unit can  
46  
47 be measured by image analysis. The numerical velocity and displacement in the same period are  
48  
49  
50 then calculated and compared with the experimental results, verifying the particle motion model.  
51  
52  
53  
54  
55  
56  
57  
58  
59  
60  
61  
62  
63  
64  
65



In each time unit, the particle acceleration is assumed to be uniform. The particle displacement in each unit is calculated by the average velocity. According to the experimental conditions, the initial conditions are

$$\begin{cases} v_{p(0)} = 0 \\ \frac{dv_p}{dt} = \frac{3\rho_f}{4d_p\rho_p} (v_f)^2 C_D \\ L_{(0)} = 0 \end{cases} \quad (4)$$

The boundary conditions are

$$\begin{cases} L_{(n1)} = L_1 \\ L_{(n2)} = L_2 \end{cases} \quad (5)$$

A specific particle is taken as an example to illustrate the verification process. This particle has a diameter of 0.647 mm and a density of 3120 kg/m<sup>3</sup>. The experimental temperature and pressure are 45.9 °C and 10.96 MPa, respectively. The SC-CO<sub>2</sub> flow rate is 1.085 m/s. The measured horizontal displacement  $L_1$  is 0.114 m, and  $L_2$  is 0.146 m. Based on the given conditions and Eqs. (1), (2), (3), (4) and (5), the numerical velocity and displacement are calculated and compared with the measured values. The results are shown in Figure 2. The straight line in Figure 2 (a) represents the velocity predicted by the particle motion model. The scattered points are the experimentally measured velocities. The higher and lower points in Figure 2 (b) are the numerical and experimental displacements of the particle, respectively. The SC-CO<sub>2</sub> displacement is used as a reference. The slippage between the SC-CO<sub>2</sub> and the particle is approximately 0.025 m. The calculated velocities and displacements have average errors of 4.90 % and 1.32 %, respectively, which match the experimental results well.

More comparisons were conducted to test the accuracy of the slippage equation, as shown in Table 2. Five particles from each group of experiments in Table 1 were randomly selected, processed

1 using the same method as described above and compared with the calculated results under the  
2  
3 same conditions. The average errors of the particle motion model are summarized in Table 2. The  
4  
5 errors are all positive values, indicating that the calculated results exceed the measurements.  
6  
7 Preliminary analysis suggests that the wall effects hinder the particle motion and slightly reduce  
8  
9 the measured particle velocities. Overall, the average velocity errors of the eight experimental  
10  
11 groups ranged from 3.48 % to 8.23 %. The average displacement errors were between 1.25 % and  
12  
13 5.49 %. Therefore, the particle motion model provides accurate predictions and can be used to  
14  
15 evaluate particle transport in SC-CO<sub>2</sub>.  
16  
17  
18  
19  
20  
21

### 22 **3.3 Derivation of the slippage velocity and displacement analytic calculations**

#### 23 **3.3.1 Neglecting the Basset force**

24  
25 To derive the analytic formulas, the effects of the Basset force on the slippage velocity and  
26  
27 displacement were analyzed. According to the measured fracture pressure gradient and the  
28  
29 geothermal gradient in the field [19,20], SC-CO<sub>2</sub> conditions of 50 MPa and 120 °C were chosen as  
30  
31 an example; these conditions are close to the underground conditions at a depth of 2000–3000 m  
32  
33 during the fracturing operation. The density and viscosity of SC-CO<sub>2</sub> under these conditions were  
34  
35 taken from the National Institute of Standards and Technology website [21] and are 763.68 kg/m<sup>3</sup>  
36  
37 and 0.068 mPa·s, respectively. The SC-CO<sub>2</sub> flow rate is assumed to be 1 m/s based on the  
38  
39 common field pump rates and fracture sizes [22]. The chosen particle density is 3120 kg/m<sup>3</sup>, and  
40  
41 the average diameter is 0.6 mm. The calculated particle velocity and displacement, with and  
42  
43 without the Basset force, are shown in Figure 3.  
44  
45  
46  
47  
48  
49  
50  
51  
52  
53

54  
55 The particle velocity differences based on the Basset force fall in the range of 2.2–6.2 %, and the  
56  
57 average value is 5.4 %, as shown in Figure 3 (a). The particle displacement differences by Basset  
58  
59  
60  
61  
62  
63  
64  
65

force in Figure 3 (b) are within the range of 0.97–5.5 %, and the average value is 4.5 %. These differences are small and can be ignored in the particle transport research. Therefore, the effects of the Basset force on the slippage velocity and displacement can be ignored.

### 3.3.2 Derivation of the horizontal velocity and slippage analytic formulas

When the Basset force is ignored, Eq. (1) becomes

$$\frac{\pi d_p^3}{6} \rho_p \frac{dv_p}{dt} = \frac{\pi d_p^2}{8} \rho_f (v_f - v_p)^2 C_D - \frac{\pi d_p^3}{12} \rho_f \frac{dv_p}{dt} \quad (6)$$

Eq. (6) can also be written as

$$\frac{dv_p}{dt} = \frac{3\rho_f C_D}{2d_p(2\rho_p + \rho_f)} (v_f - v_p)^2 \quad (7)$$

Letting

$$T_r = \frac{2d_p(2\rho_p + \rho_f)}{3\rho_f C_D} \quad (8)$$

Then, Eq. (7) can then be simplified to

$$(v_f - v_p)^{-2} dv_p = \frac{1}{T_r} dt \quad (9)$$

The drag coefficient ( $C_D$ ) is solved by Eq. (2) and is a constant value under certain pressure and temperature conditions according to the previous study on particle settling in SC-CO<sub>2</sub> [15].

Therefore, Eq. (9) can be integrated directly. The initial particle horizontal velocity is assumed to be zero. The slippage velocity ( $S_V$ ) is calculated as

$$S_V = v_f - v_p = \frac{T_r \cdot v_f}{t \cdot v_f + T_r} \quad (10)$$

The slippage displacement ( $S_D$ ), defined as the relative displacement between the particle and the SC-CO<sub>2</sub> in the horizontal direction, can be derived based on Eq. (10)

$$S_D = v_f \cdot t - \int_0^t v_p dt \quad (11)$$

By combining Eqs. (10) and (11), the slippage displacement equation is given by

$$S_D = T_r \cdot \ln\left(\frac{v_f \cdot t + T_r}{T_r}\right) \quad (12)$$

Eqs. (10) and (12) are the first analytic solutions for particle slippage velocity and displacement in SC-CO<sub>2</sub>, which can be applied for the particle-SC-CO<sub>2</sub> two-phase flow analysis in particle tracing, fluidization, transportation, etc.

### 3.4 Numerical analysis of particle relative motion in SC-CO<sub>2</sub>

The particle-SC-CO<sub>2</sub> slippage was analyzed using the slippage velocity and displacement calculations. The most widely used ceramicsite was chosen as the particle type and has a density of 3120 kg/m<sup>3</sup>. The particle diameter was 0.6 mm, which is the average value of the commonly used proppant.

#### 3.4.1 Flow rate effects on the particle-SC-CO<sub>2</sub> slippage

The slippage velocity and displacement under various SC-CO<sub>2</sub> flow rate conditions are shown in Figure 4. The pressure and temperature conditions of the SC-CO<sub>2</sub> were 50 MPa and 120 °C, which are close to the underground conditions at a depth between 2000 m and 3000 m during the fracturing operation. The practical flow rate in actual underground fractures is determined by the pump rate, fracture size, leak off, etc. Hence, the flow rates used in the evaluation were in the range from 0.5–2.5 m/s [22].

The slippage velocity decreases rapidly with increasing particle velocity. After 0.15 s, the slippage velocity decreases extremely slowly. Different flow rates have little effect on the slippage velocity, as shown in Figure 4 (a).

1 The slippage displacement is the accumulated relative displacement between the particle and the  
2  
3 SC-CO<sub>2</sub>. In the early stage (before 10 s), slippage displacement increases rapidly, as shown in  
4  
5 Figure 4 (b). The increasing rate then drops with decreasing slippage velocity, and the curve  
6  
7 becomes a straight line with a small slope. All of the slippage displacements are at the centimeter  
8  
9 level and far below the underground fracture length in formation, which is typically at the  
10  
11 ten-meter or even hundred-meter level [23]. Thus, the relative displacement between the  
12  
13 proppant and SC-CO<sub>2</sub> is negligible in field applications, where the proppant is transported deep  
14  
15 into the fracture along the length direction. SC-CO<sub>2</sub> is proven to be qualified for proppant  
16  
17 transport in the horizontal direction under various flow rate conditions.  
18  
19  
20  
21  
22  
23

#### 24 25 **3.4.2 Effects of SC-CO<sub>2</sub> density and viscosity on slippage**

26  
27 Similar to the effect of the flow rate on the slippage velocity, the effects of the SC-CO<sub>2</sub> density  
28  
29 and viscosity on the slippage velocity are inconspicuous. Therefore, only the slippage  
30  
31 displacement was analyzed, as shown in Figure 5. The slippage displacements decrease with  
32  
33 increasing SC-CO<sub>2</sub> density and viscosity. Even under relatively low density (300 kg/m<sup>3</sup>) and  
34  
35 viscosity (0.01 mPa·s) conditions, the slippage displacements are all at the centimeter level and  
36  
37 less than 0.08 m, which demonstrates the particle transport ability of SC-CO<sub>2</sub>.  
38  
39  
40  
41  
42  
43

44 Two interesting differences were discovered between Figure 5 (a) and Figure 5 (b). One  
45  
46 difference is that a viscosity increase of a factor of ten thousand reduces the slippage from 0.08  
47  
48 m to 0.04 m, while a density increase of a factor of less than four reduces the slippage by the  
49  
50 same amount. The other difference is that the reduction rate of the slippage decreases with  
51  
52 increasing viscosity, while the reduction rate increases with increasing density. In Figure 5 (a),  
53  
54 the slippage reduces slightly when the SC-CO<sub>2</sub> density increases from 300 kg/m<sup>3</sup> to 500 kg/m<sup>3</sup>.  
55  
56  
57  
58  
59  
60  
61  
62  
63  
64  
65

1 However, the slippage **decreases by** 50 % (from approximately 0.06 m to 0.03 m) when the  
 2  
 3 density increases from 900  $\text{kg/m}^3$  to 1100  $\text{kg/m}^3$ . In **Figure 5** (b), the effect of **the** SC-CO<sub>2</sub>  
 4  
 5 viscosity follows a reverse rule in which the reduction rate of the slippage decreases with  
 6  
 7 increasing viscosity.  
 8  
 9

10  
 11 Past research views the viscosity as the main physical criterion of fracturing fluids for proppant  
 12  
 13 transport because **a** high viscosity prevents the proppant from settling in the vertical direction.  
 14  
 15 However, the above analysis reveals that the density of SC-CO<sub>2</sub> exerts a greater influence on  
 16  
 17 particle slippage than the viscosity. The density of SC-CO<sub>2</sub>, rather than only the viscosity, should  
 18  
 19 be evaluated for effective proppant transport.  
 20  
 21  
 22  
 23

### 24 **3.4.3 Comparison of the slippage in SC-CO<sub>2</sub> and water**

25  
 26 The slippage velocity and displacement in SC-CO<sub>2</sub> and water were compared. The density and  
 27  
 28 viscosity of water are 1000  $\text{kg/m}^3$  and 1 mPa·s, respectively. The particle diameter and density  
 29  
 30 are 0.6 mm and 3120  $\text{kg/m}^3$ , respectively. The pressure and temperature of SC-CO<sub>2</sub> **are** 50 MPa  
 31  
 32 and 120 °C, respectively. The fluid flow rates are both 1 m/s.  
 33  
 34  
 35  
 36  
 37  
 38

39 For water, Eq. (2) is unsuitable for the drag coefficient solution. Instead, the Stokes drag  
 40  
 41 coefficient equation ( $C_D=24 / Re$ ) is applied [24]. The slippage equations for water are given by  
 42  
 43

$$44 \begin{cases} S_{Vw} = e^{-\frac{t}{T_{rw}}} v_{fw} \\ S_{Dw} = v_{fw} T_{rw} (1 - e^{-\frac{t}{T_{rw}}}) \end{cases} \quad (13)$$

45  
 46  
 47  
 48  
 49  
 50  
 51 where

$$52 \quad T_{rw} = \frac{d^2 (2\rho_p + \rho_{fw})}{36\mu_w} \quad (14)$$

53  
 54  
 55  
 56  
 57  
 58  
 59  
 60  
 61  
 62  
 63  
 64  
 65

1 The comparison results, which were calculated using Eqs. (8), (10), (12), (13) and (14), are  
2  
3 shown in Figure 6. Both of the slippage velocities in SC-SO<sub>2</sub> and water exhibited nearly the same  
4  
5 rate of decrease. The main difference was that the slippage velocity rapidly decreased to zero in  
6  
7 water, whereas it decreased at an extremely slow rate after a sharp decrease and did not decrease  
8  
9 to zero in SC-CO<sub>2</sub> (Fig. 6 (a)). This difference indicates that particles flowing with water can  
10  
11 reach the water flow velocity, although they cannot reach the flow velocity when flowing with  
12  
13 SC-CO<sub>2</sub>.

14  
15  
16  
17  
18  
19  
20 The slippage displacement reflects the corresponding slippage velocity law, as shown in Figure 6  
21  
22 (b). The slippage displacement in the water increased rapidly to a constant value because the  
23  
24 slippage velocity in water can decrease to zero. However, the slippage displacement curve in  
25  
26 SC-CO<sub>2</sub> approached a straight line with a small slope because the slippage velocity always exists  
27  
28 and the slippage displacement continually increases, even after 100 s.

29  
30  
31  
32  
33 Although the experiments conducted here demonstrated the superior particle transporting  
34  
35 capability of SC-CO<sub>2</sub> and showed that it is similar to a liquid, the additional numerical analysis  
36  
37 revealed the detailed differences in the slippage velocity and displacement between SC-CO<sub>2</sub> and  
38  
39 water. However, it is worth noting that the differences in the slippage velocities (less than 10 % of  
40  
41 the flowing velocity) and displacements (centimeter level) are relatively insignificant and  
42  
43 negligible under the conditions of petroleum engineering applications. In addition, the vertical  
44  
45 particle motion also indicated that the particle settling velocity in SC-CO<sub>2</sub> was similar to that for  
46  
47 liquid CO<sub>2</sub> [15]. By synthesizing the horizontal and vertical particle motion characteristics in  
48  
49 SC-CO<sub>2</sub>, the conclusion that SC-CO<sub>2</sub> has superior particle transporting capability is emphasized.

#### 50 51 52 53 54 55 56 57 58 **4 Conclusions**

1 In this work, experimental and numerical methods were applied to study the slippage in  
2  
3 particle-SC-CO<sub>2</sub> two-phase flow. The experimentally measured slippage velocity (10.3 % of the  
4  
5 SC-CO<sub>2</sub> flowing rate) and displacement (centimeter level) indicated that SC-CO<sub>2</sub> has a superior  
6  
7 particle transporting capability that is similar to those of liquids. The analytic calculations for the  
8  
9 slippage velocity and displacement of SC-CO<sub>2</sub> were derived and applied for additional numerical  
10  
11 analyses. The density of SC-CO<sub>2</sub> was found to have a greater influence on particle slippage than  
12  
13 the viscosity. Hence, the density of SC-CO<sub>2</sub>, rather than only the viscosity, should be evaluated for  
14  
15 effective particle transport. A comparison of the slippage between SC-CO<sub>2</sub> and water revealed that  
16  
17 both of the slippage evolution had approximately the same behavior. However, the slippage  
18  
19 velocity in water approached zero, while it continually decreased at an extremely slow rate after  
20  
21 the same sharp decrease in SC-CO<sub>2</sub>. Thus, the slippage displacement in water tended to be  
22  
23 constant, while it continually increased at an extremely slow rate in SC-CO<sub>2</sub>. These differences in  
24  
25 the slippage velocity (less than 10 % of the flowing velocity) and displacement (centimeter level)  
26  
27 are relatively insignificant and negligible under the conditions of engineering applications.  
28  
29  
30  
31  
32  
33  
34  
35  
36  
37  
38

### 39 Acknowledgements

40 This work was supported by the Natural Science Foundation of China (U1262202, 5121006)

### 44 Appendix

47	$d_p$	[m]	diameter of the particle
48	$\rho_p$	[kg/m <sup>3</sup> ]	density of the particle
49	$v_p$	[m/s]	horizontal velocity of the particle
50	$\rho_f$	[kg/m <sup>3</sup> ]	SC-CO <sub>2</sub> density
51	$\rho_{fw}$	[kg/m <sup>3</sup> ]	water density
52			
53			
54			
55			
56			
57			
58			
59			
60			
61			
62			
63			
64			
65			



1	$v_f$	[m/s]	SC-CO <sub>2</sub> flow rate
2			
3	$v_{fw}$	[m/s]	water flow rate
4			
5			
6	$\mu$	[Pa·s]	SC-CO <sub>2</sub> viscosity
7			
8			
9	$\mu_w$	[Pa·s]	water viscosity
10			
11	$t, \tau$	[s]	time
12			
13			
14	$C_D$	[-]	drag coefficient
15			
16			
17	$v_\infty$	[m/s]	terminal settling velocity of particle in SC-CO <sub>2</sub>
18			
19			
20	$g$	[m/s <sup>2</sup> ]	gravity
21			
22	$Ar$	[-]	particle Archimedes number, $Ar = \frac{g(\rho_p - \rho_f)\rho_f d_p^3}{\mu^2}$
23			
24			
25	$h$	[s]	time unit
26			
27			
28	$a_i, a_j$	[m/s <sup>2</sup> ]	particle horizontal acceleration at different moments
29			
30			
31	$v_{p(i)}$	[m/s]	particle horizontal velocity at moment $t_i$
32			
33			
34	$L_1, L_2, L_{(i)}$	[m]	particle horizontal displacement at different moments
35			
36			
37	$T_r, T_{rw}$	[-]	procedure parameter of formula derivation
38			
39	$S_V$	[m/s]	slippage velocity between the particle and SC-CO <sub>2</sub>
40			
41			
42	$S_D$	[m]	slippage displacement between the particle and SC-CO <sub>2</sub>
43			
44			
45	$S_{Vw}$	[m/s]	slippage velocity between the particle and water
46			
47			
48	$S_{Dw}$	[m]	slippage displacement between the particle and water
49			
50			
51	$e$	[-]	Napierian logarithm
52			
53	$T$	[°C]	temperature of SC-CO <sub>2</sub>
54			
55			
56	$P$	[MPa]	pressure of SC-CO <sub>2</sub>
57			

## References

- 1 [1] L. Zhang, S. Ren, B. Ren, W. Zhang, Q. Guo, L. Zhang, Assessment of CO<sub>2</sub> storage  
2 capacity in oil reservoirs associated with large lateral/underlying aquifers: case studies  
3 from China, *Int. J. Greenhouse Gas Contr.* 5 (2011) 1016-1021.  
4  
5  
6  
7  
8  
9 [2] B. Ren, L. Zhang, H. Huang, S. Ren, G. Chen, H. Zhang, Performance evaluation and  
10 mechanisms study of near-miscible CO<sub>2</sub> flooding in a tight oil reservoir of Jilin oilfield  
11 China, *J. Nat. Gas Sci. Eng.* 27 (2015) 1796-1805.  
12  
13  
14  
15  
16  
17 [3] R.A. Chadwick, D.J. Noy, S. Holloway, Flow processes and pressure evolution in aquifers  
18 during the injection of supercritical CO<sub>2</sub> as a greenhouse gas mitigation measure, *Petrol.*  
19  
20  
21  
22  
23  
24  
25  
26 [4] G. Zhang, C. Taberner, L. Cartwright, T. Xu, Injection of supercritical CO<sub>2</sub> into deep saline  
27 carbonate formations: predictions from geochemical modeling, *SPE J.* 16 (2011) 959–967.  
28  
29  
30  
31 [5] C.G. Street, C. Tesche, S. Guigard, Treatment of hydrocarbon-based drilling waste using  
32 supercritical carbon dioxide, *SPE Drill. Completion* 9 (2009) 413–417.  
33  
34  
35  
36 [6] R. Khanpour, M.R. Sheikhi-Kouhsar, F. Esmaeilzadeh, D. Mowla, Removal of  
37 contaminants from polluted drilling mud using supercritical carbon dioxide extraction, *J.*  
38  
39  
40  
41  
42  
43  
44  
45 [7] Y.K. Du, R.H. Wang, H.J. Ni, H.J. Huo, Z.Y. Huang, W.M. Yue, H.X. Zhao, B. Zhao,  
46  
47  
48  
49  
50  
51  
52  
53 [8] Y. Du, R. Wang, H. Ni, M. Li, W. Song, H. Song, Determination of rock-breaking  
54  
55  
56  
57  
58  
59  
60  
61  
62  
63  
64  
65 performance of high-pressure supercritical carbon dioxide jet, *J. Hydrodynamics B* 24  
(2012) 554–560.

- 1 [9] B. Sun, Y. Zhang, Q. Du, Z. Shen, Property evaluation of CO<sub>2</sub> adsorption and desorption  
2  
3 on shale, *J. Chin. Univ. Petrol.* 37 (2013) 95-99.  
4  
5
- 6 [10] T. Wu, Q. Xue, X. Li, Y. Tao, Y. Jin, C. Ling, S. Lu, Extraction of kerogen from oil shale  
7  
8 with supercritical carbon dioxide: molecular dynamics simulations, *J. Supercrit. Fluids* 107  
9  
10 (2016) 499–506.  
11  
12
- 13 [11] Z. Wang, B. Sun, J. Wang, L. Hou, Experimental study on the friction coefficient of  
14  
15 supercritical carbon dioxide in pipes, *Int. J. Greenhouse Gas Contr.* 25 (2014) 151–161.  
16  
17
- 18 [12] Z. Wang, B. Sun, L. Yan, Improved density correlation for supercritical CO<sub>2</sub>, *Chem. Eng.*  
19  
20 *Technol.* 38 (2015) 75–84.  
21  
22
- 23 [13] N.A. Patankar, D.D. Joseph, J. Wang, R.D. Barree, M. Conway, M. Asadi, Power law  
24  
25 correlations for sediment transport in pressure driven channel flows, *Int. J. Multiphase*  
26  
27 *Flow* 28 (2002) 1269–1292.  
28  
29
- 30 [14] M.A. Biot, W.L. Medlin, *Theory of Sand Transport in Thin Fluids*, SPE, 1985, p. 14468.  
31  
32
- 33 [15] L. Hou, B. Sun, Z. Wang, Q. Li, Experimental study of particle settling in supercritical  
34  
35 carbon dioxide, *J. Supercrit. Fluids* 100 (2015) 121–128.  
36  
37
- 38 [16] E.E. Michaelides, Review: transient equation of motion for particles, bubbles, and droplets,  
39  
40 *J. Fluids Eng.* 119 (1997) 233–247.  
41  
42
- 43 [17] H. Shehua, L. Wei, C. Liangjun, On numerical method of resolving discrete solid particles  
44  
45 motion equation and its applications, *J. Hydrodynamics* 14 (1999) 51–61.  
46  
47
- 48 [18] F.A. Bombardelli, A.E. González, Y.I. Niño, Computation of the particle basset force with  
49  
50 a fractional-derivative approach, *J. Hydraul. Eng.* 134 (2008) 1513–1519.  
51  
52
- 53 [19] N.C. Dutta, Geopressure prediction using seismic data: Current status and the road ahead,  
54  
55  
56  
57  
58  
59  
60  
61  
62  
63  
64  
65

1 Geophysics 67 (2002) 2012–2041.

- 2
- 3 [20] S. Cao, I. Lerche, Geohistory, thermal history and hydrocarbon generation history of
- 4
- 5
- 6 Navarin Basin COST No.1 well Bering Sea Alaska, *J. Petrol. Geol.* 12 (1989) 325–352.
- 7
- 8
- 9 [21] National Institute of Standards and Technology, NIST, Chemistry WebBook, 2014.
- 10
- 11 <http://webbook.nist.gov/chemistry/fluid/>.
- 12
- 13
- 14 [22] J. Micheal, Economides, in: *Reservoir Stimulation*, Petroleum Industry Press, Beijing, 3rd
- 15
- 16 ed., (2002), pp. 145–151.
- 17
- 18
- 19 [23] X.E. Refunjol, K.M. Keranen, J.H. Le Calvez, K.J. Marfurt, Integration of hydraulically
- 20
- 21
- 22 induced microseismic event locations with active seismic attributes: A North Texas Barnett
- 23
- 24
- 25 Shale case study, *Geophysics* 77 (2012) KS1–KS12.
- 26
- 27
- 28 [24] E. Novotny, Proppant transport, in: *Proceedings of the 52nd Annual Fall Technical*
- 29
- 30
- 31 *Conference and Exhibition of the Society of Petroleum Engineers*, Vol. 2, Denver, 9-12
- 32
- 33
- 34
- 35
- 36
- 37
- 38
- 39
- 40
- 41
- 42
- 43
- 44
- 45
- 46
- 47
- 48
- 49
- 50
- 51
- 52
- 53
- 54
- 55
- 56
- 57
- 58
- 59
- 60
- 61
- 62
- 63
- 64
- 65



## Figure List




Fig. 1 Schematic of the visualization channel simulator and high-speed camera system.

Fig. 2 Comparisons of the velocities and displacements from the measured and numerical results.

The particle density and diameter are  $3120 \text{ kg/m}^3$  and  $0.647 \text{ mm}$ , respectively. The temperature, pressure and flow rate of SC-CO<sub>2</sub> are  $45.9 \text{ }^\circ\text{C}$ ,  $10.96 \text{ MPa}$  and  $1.085 \text{ m/s}$ , respectively. (a)

Comparison of the velocities from the measured and numerical results in the observation window

range. The middle linear points  represent the numerical results, and the scattered points  represent the measured results. (b) Comparison of the displacements from the measured and

numerical results in the observation window range. The upper points  represent the calculated SC-CO<sub>2</sub> displacement, which is used as a reference. The middle points  represent the numerical particle displacement, and the lower points  represent the experimental particle displacement.






numerical results in the observation window range. The upper points  represent the calculated SC-CO<sub>2</sub> displacement, which is used as a reference. The middle points  represent the numerical particle displacement, and the lower points  represent the experimental particle displacement.

Fig. 3 Calculated particle velocity and displacement with and without Basset force. The particle density and diameter are  $3120 \text{ kg/m}^3$  and  $0.6 \text{ mm}$ , respectively. The temperature, pressure and flow rate of SC-CO<sub>2</sub> are  $120 \text{ }^\circ\text{C}$ ,  $50 \text{ MPa}$  and  $1 \text{ m/s}$ , respectively. (a) Calculated particle velocity with and

without Basset force. The upper points  represent the calculated particle velocity without Basset force. The lower points  represent the calculated particle velocity with Basset force. (b)




Calculated particle displacement with and without Basset force. The upper points  represent the calculated SC-CO<sub>2</sub> displacement, which is used as a reference. The middle points  represent the calculated particle displacement without Basset force, and the lower points  represent the calculated particle displacement with Basset force.

Fig. 4 Particle slippage velocity and displacement in SC-CO<sub>2</sub> under various flow rate conditions. The particle density and diameter are 3120 kg/m<sup>3</sup> and 0.6 mm, respectively. The temperature and pressure of SC-CO<sub>2</sub> are 120 °C and 50 MPa, respectively. (a) Particle slippage velocity in SC-CO<sub>2</sub> under various flow rate conditions. The flow rates from top to bottom are 2.5 m/s ■, 2.0 m/s ●, 1.5 m/s ▲, 1.0 m/s ▼ and 0.5 m/s ◆. (b) Particle slippage displacement in SC-CO<sub>2</sub> under various flow rate conditions. The flow rates from top to bottom are 2.5 m/s ■, 2.0 m/s ●, 1.5 m/s ▲, 1.0 m/s ▼ and 0.5 m/s ◆.

Fig. 5 Particle slippage displacement under various SC-CO<sub>2</sub> density and viscosity conditions. The particle density and diameter are 3120 kg/m<sup>3</sup> and 0.6 mm, respectively. (a) Particle slippage displacement under various SC-CO<sub>2</sub> density conditions. The viscosity and flow rate of SC-CO<sub>2</sub> are 0.068 mPa·s and 1 m/s, respectively. The SC-CO<sub>2</sub> densities from top to bottom are 300 kg/m<sup>3</sup> ■, 500 kg/m<sup>3</sup> ●, 700 kg/m<sup>3</sup> ▲, 900 kg/m<sup>3</sup> ▼ and 1100 kg/m<sup>3</sup> ◆. (b) Particle slippage displacement under various SC-CO<sub>2</sub> viscosity conditions. The density and flow rate of SC-CO<sub>2</sub> are 763.68 kg/m<sup>3</sup> and 1 m/s, respectively. The SC-CO<sub>2</sub> viscosities from top to bottom are 0.01 mPa·s ■, 0.1 mPa·s ●, 1.0 mPa·s ▲, 10.0 mPa·s ▼ and 100.0 mPa·s ◆.

Fig. 6 Comparison of the particle slippage velocity and displacement in SC-CO<sub>2</sub> and water. The particle density and diameter are 3120 kg/m<sup>3</sup> and 0.6 mm, respectively. The temperature and pressure of SC-CO<sub>2</sub> are 120 °C and 50 MPa, respectively. The density and viscosity of water are 1000 kg/m<sup>3</sup> and 1 mPa·s, respectively. The flow rates are both 1 m/s. (a) Comparison of the particle slippage velocity in SC-CO<sub>2</sub> and water. The ■ points represent the slippage velocities in SC-CO<sub>2</sub>,

and the ● points represent the slippage velocities in water. (b) Comparison of the particle slippage displacement in SC-CO<sub>2</sub> and water. The upper points ■ represent the slippage displacements in SC-CO<sub>2</sub>, and the lower points ● represent the slippage displacements in water.

Figure 1  
[Click here to download high resolution image](#)

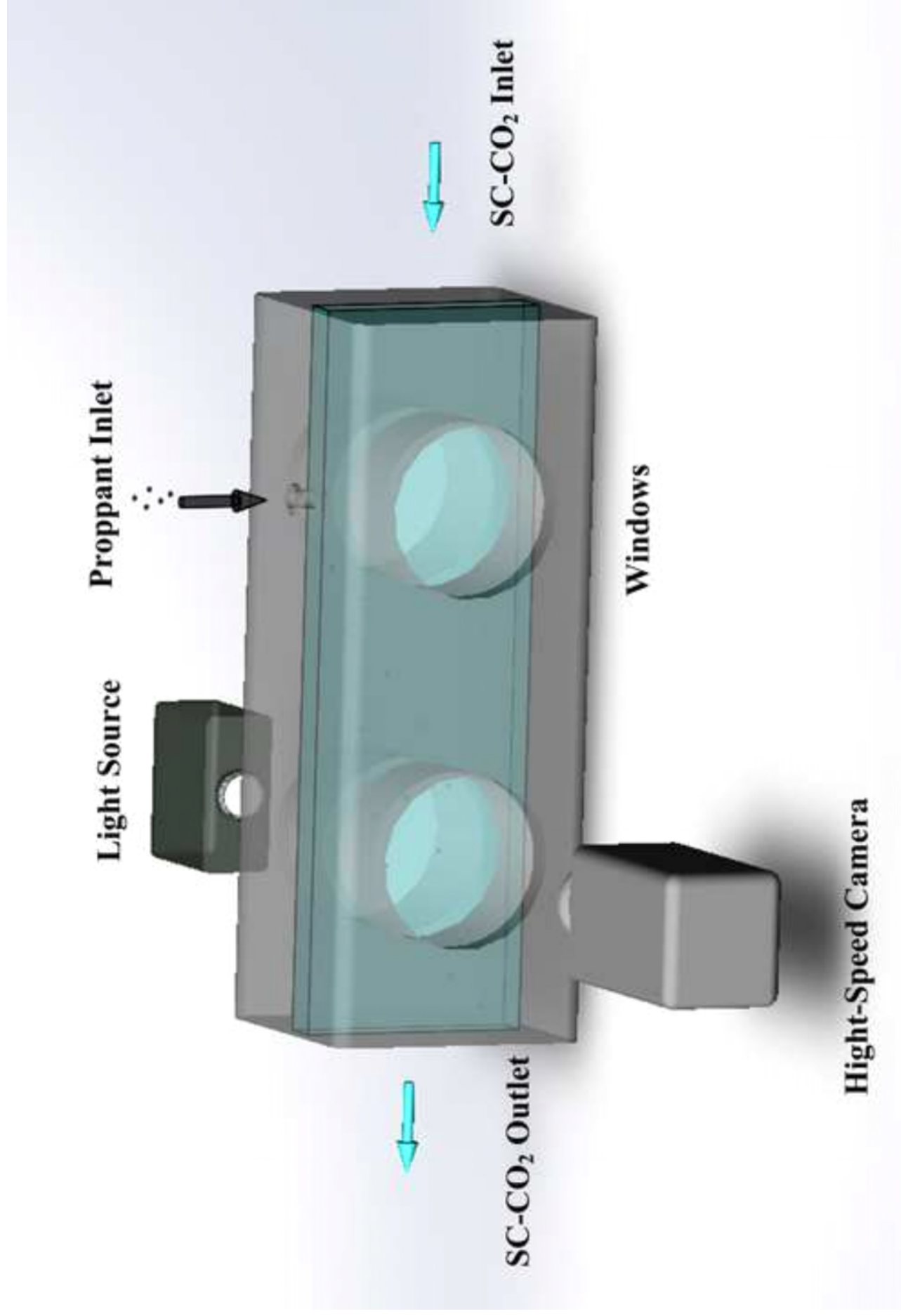




Figure 2 (a)

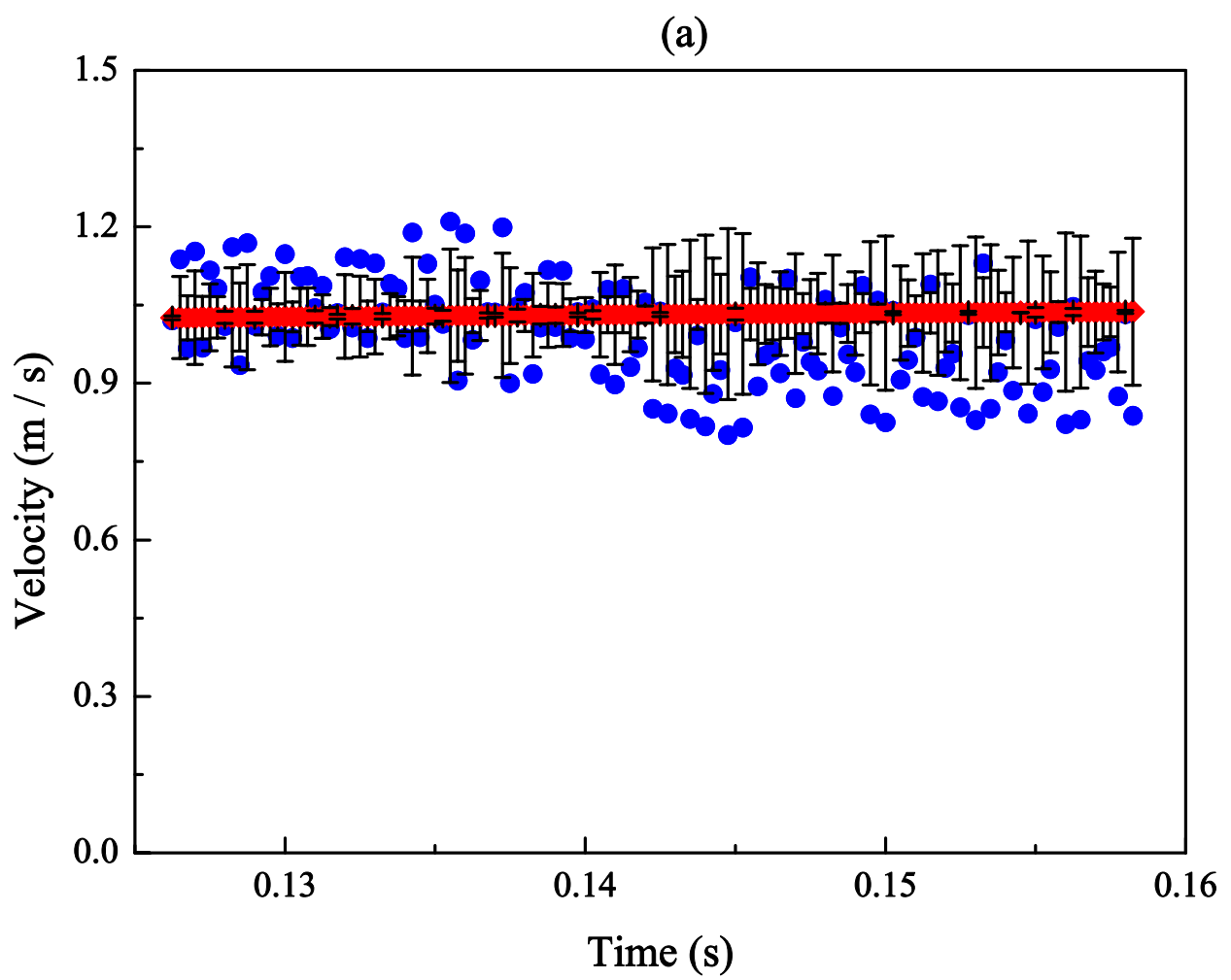


Figure 2 (b)

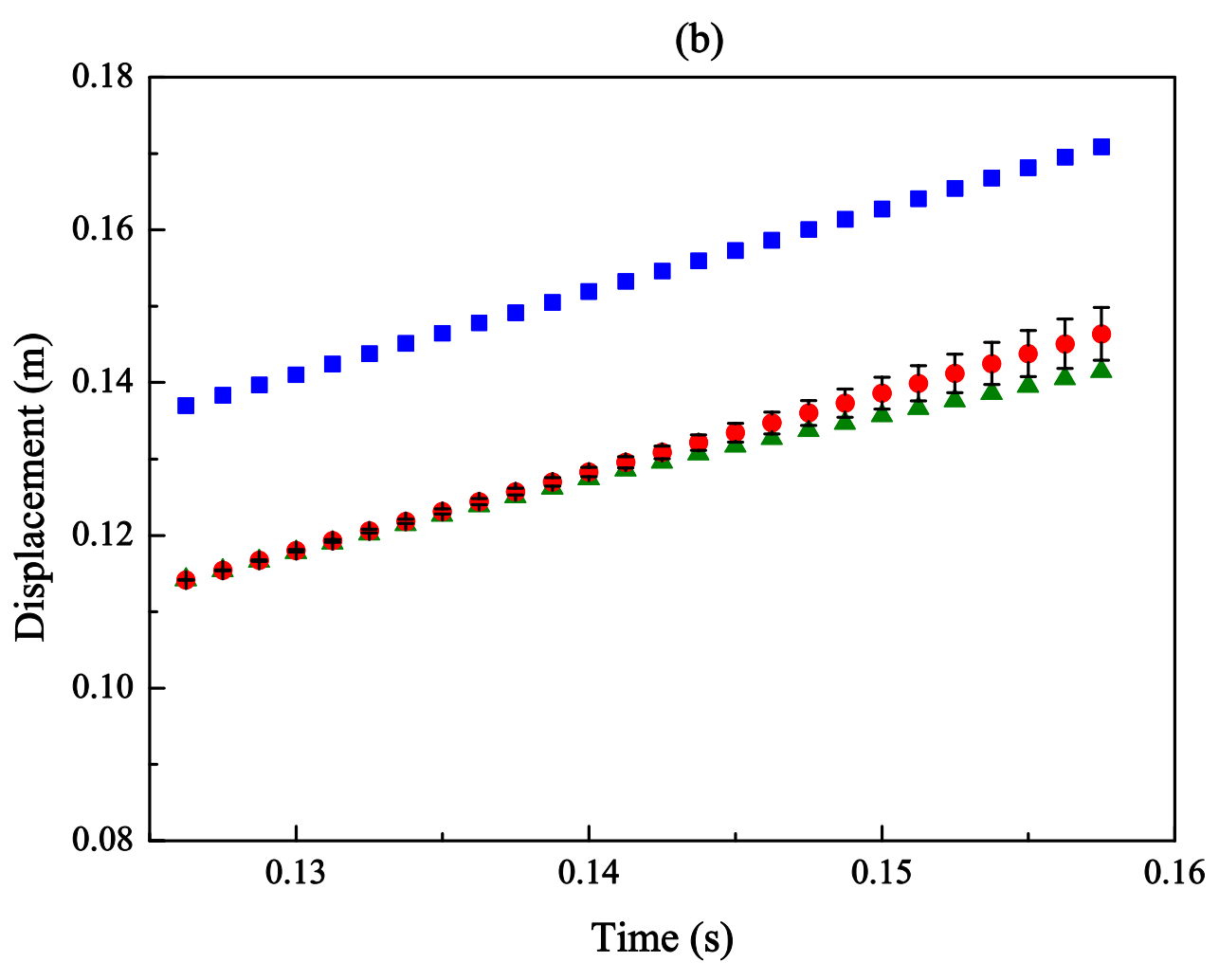


Figure 3 (a)

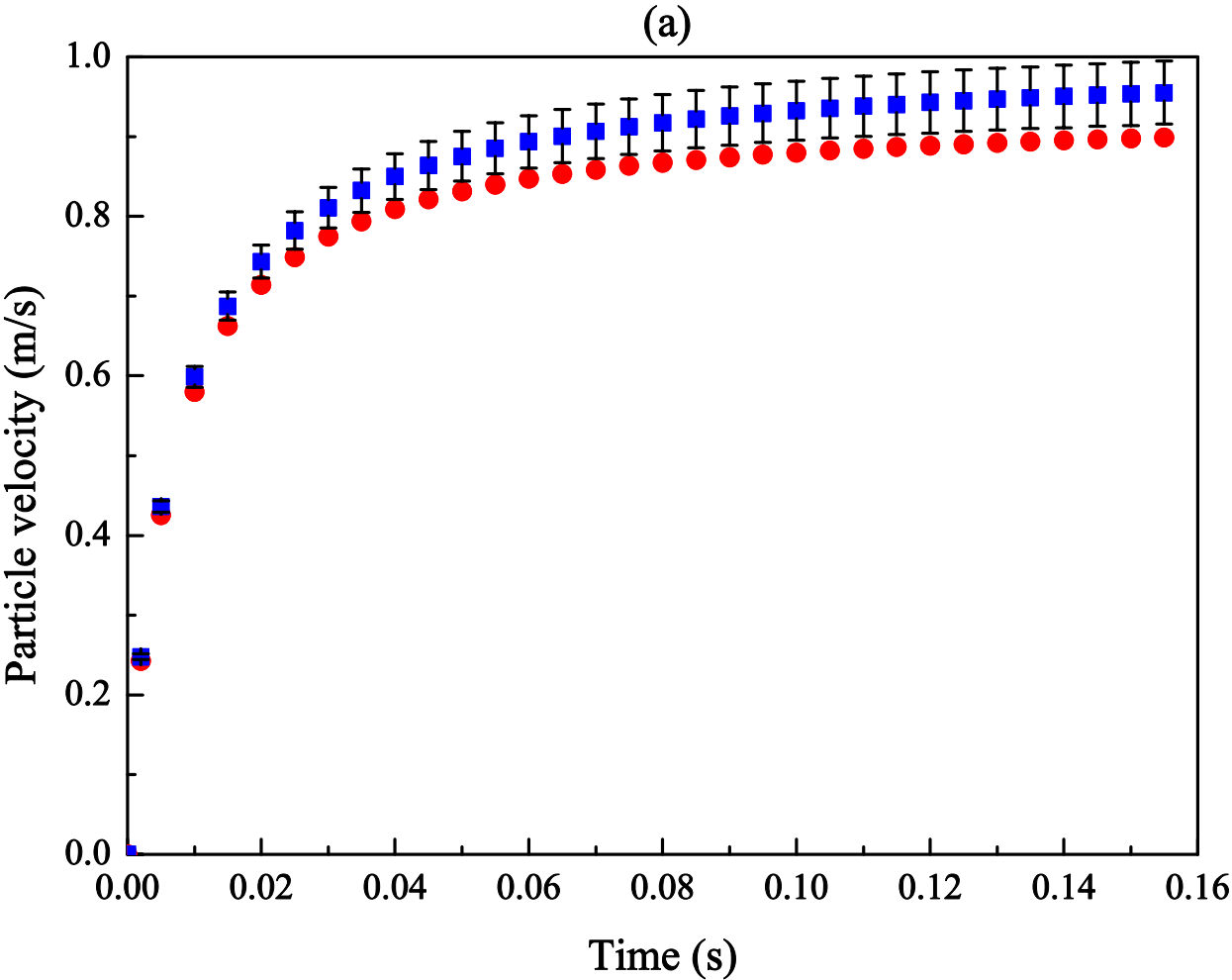


Figure 3 (b)

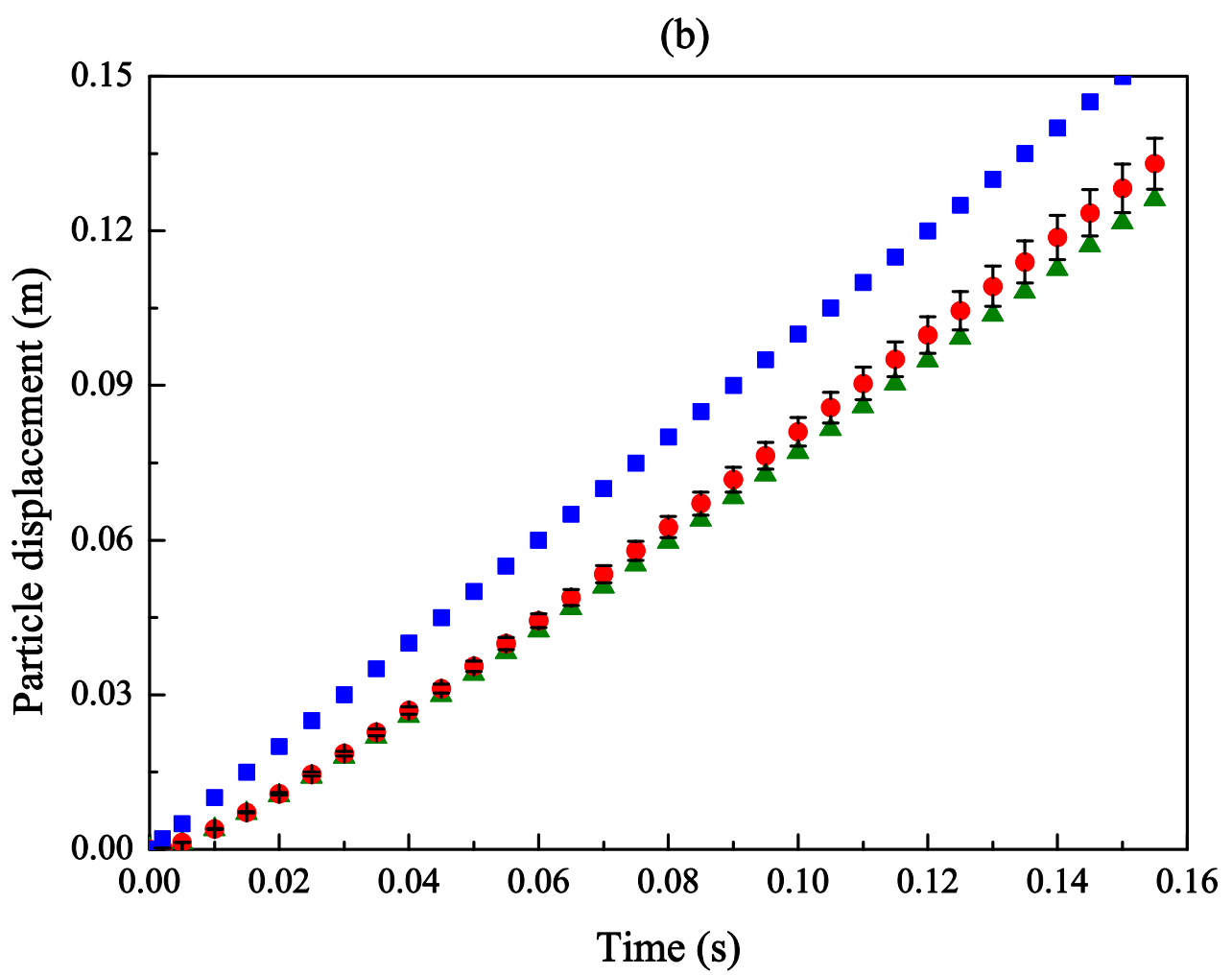


Figure 4 (a)

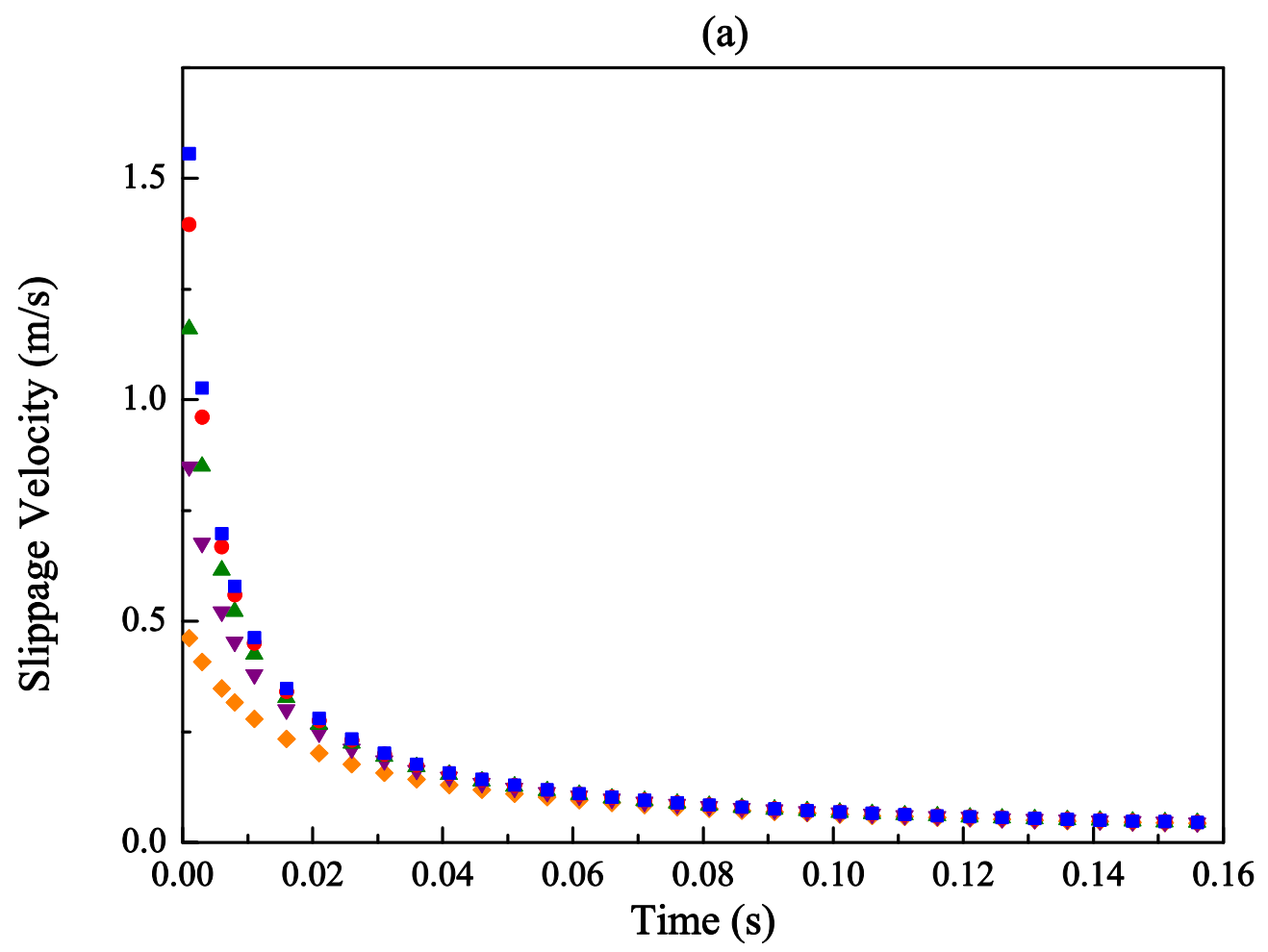


Figure 4 (b)

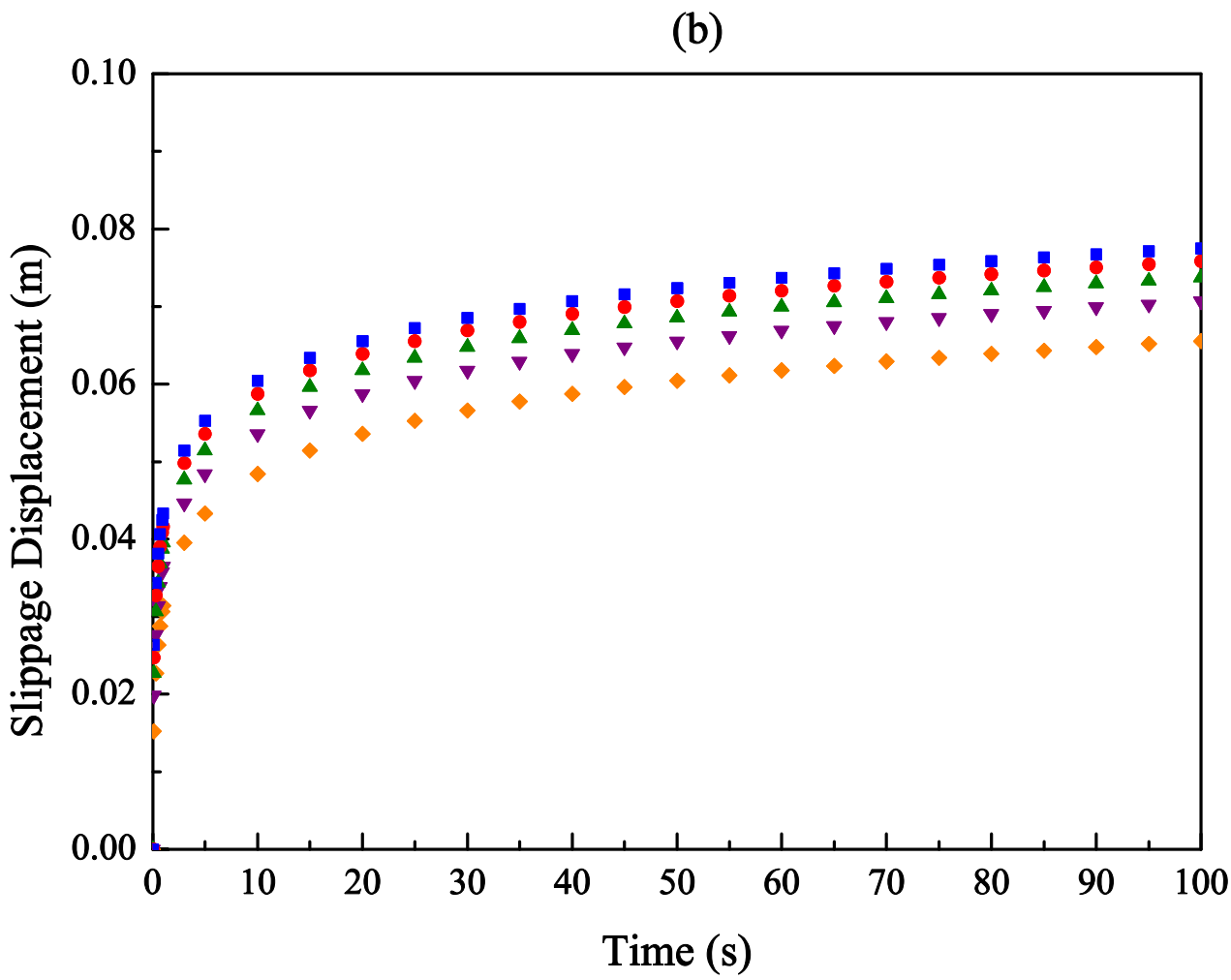


Figure 5 (a)

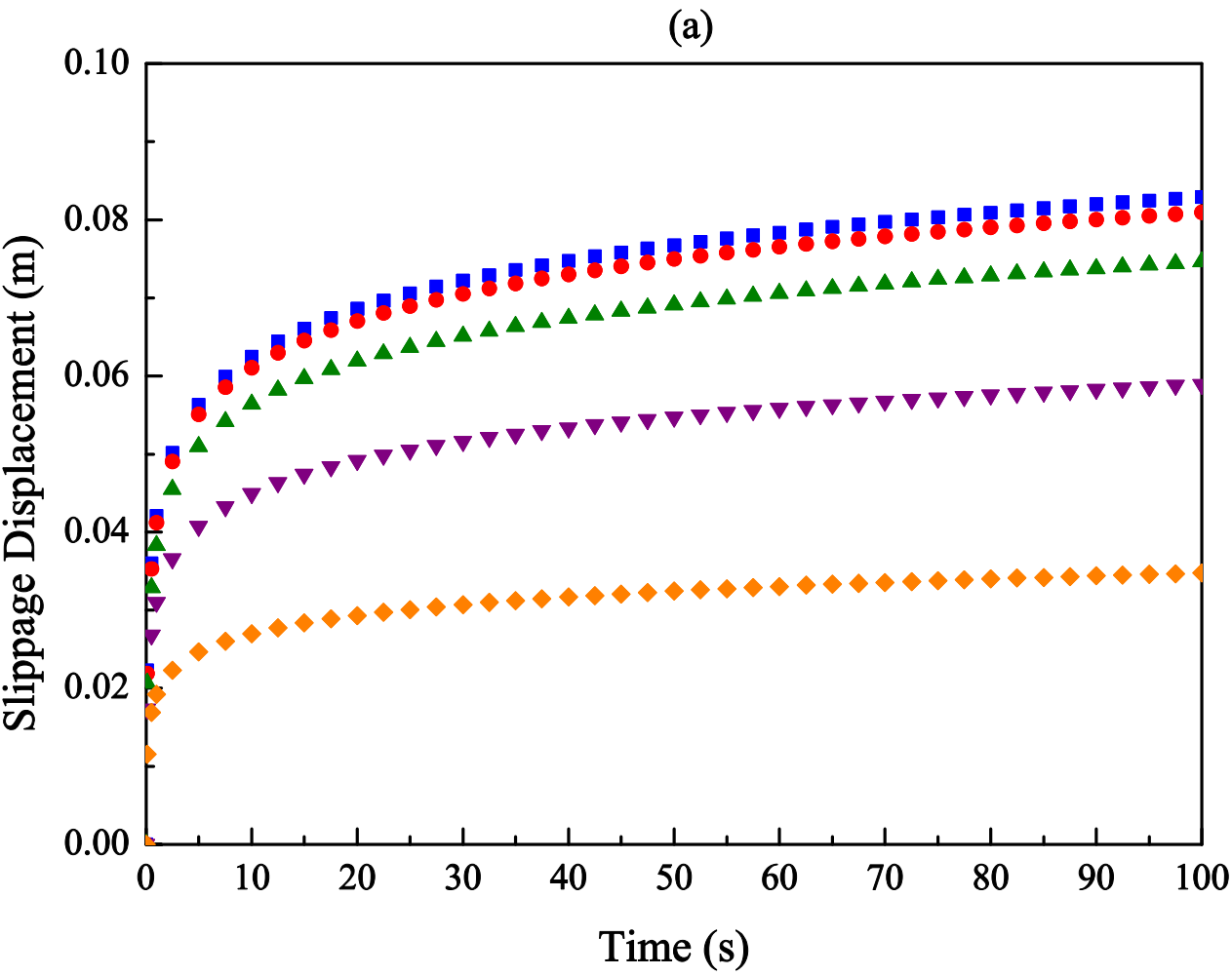


Figure 5 (b)

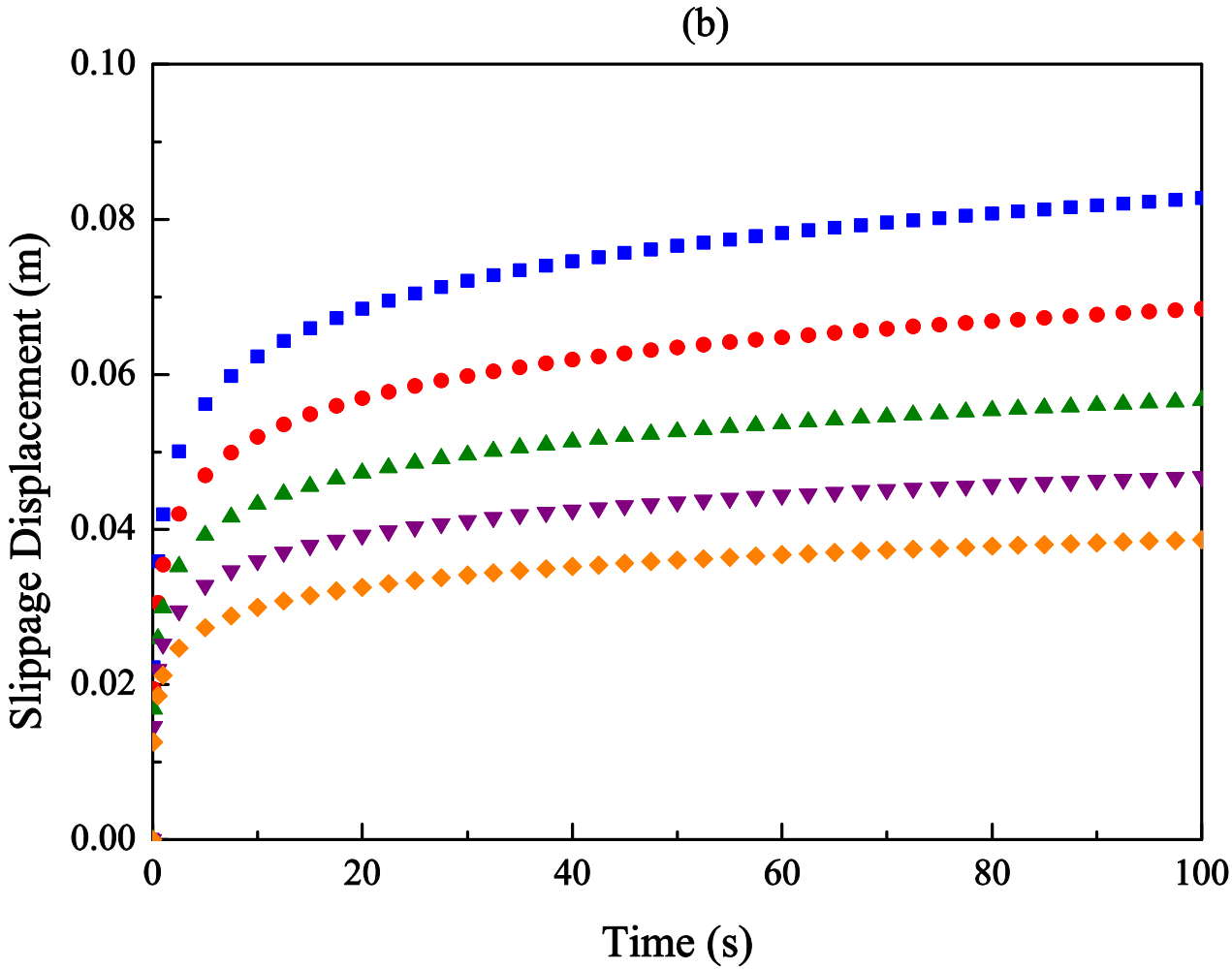




Figure 6 (a)

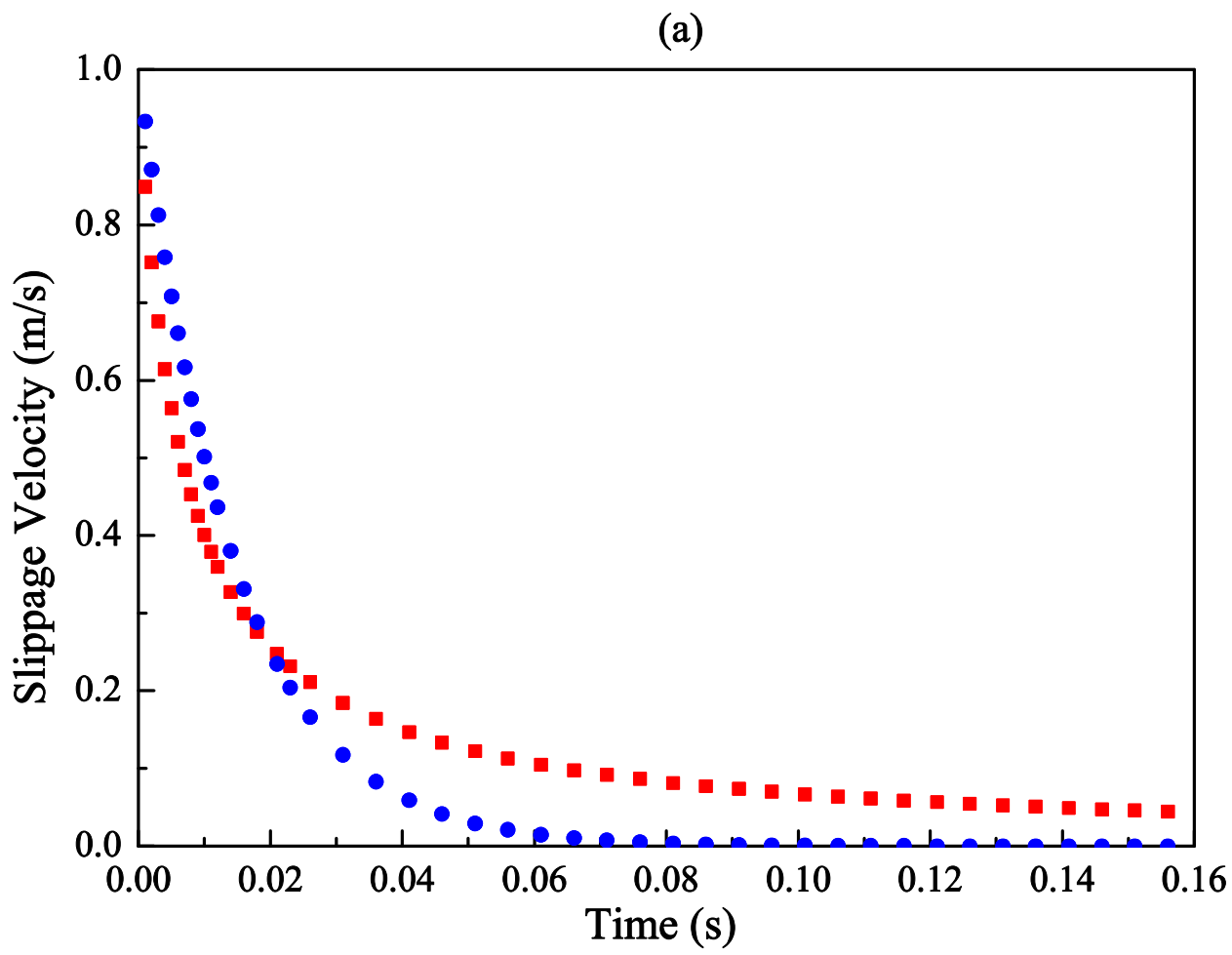


Figure 6 (b)

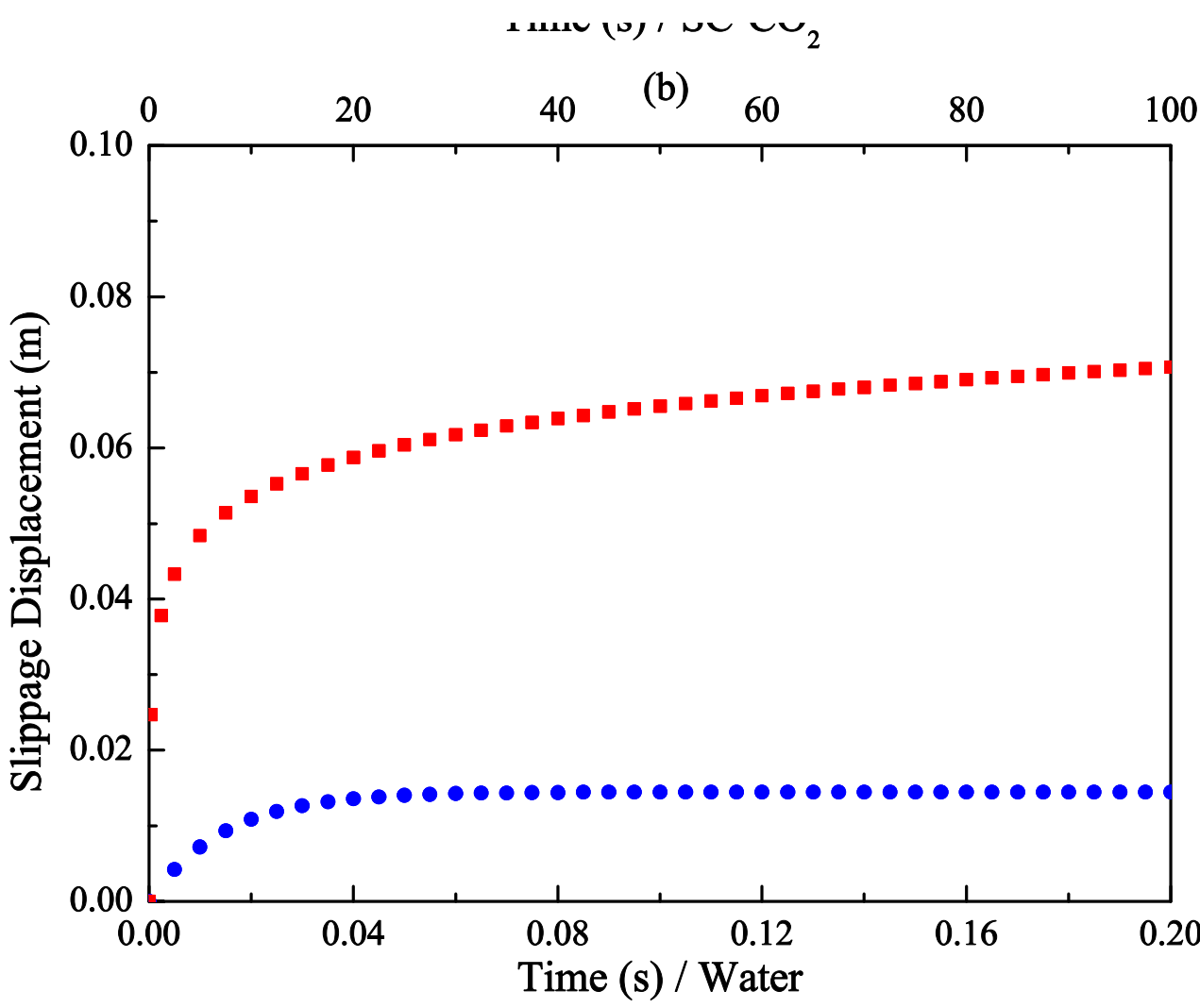


Table 1

## Experimental measured particle average velocity and slippage displacement

No.	Proppant condition		SC-CO <sub>2</sub> condition			Average particle velocity m/s	Average slippage displacement m
	$\rho_p / \text{kg/m}^3$	$d_p / \text{mm}$	$T / ^\circ\text{C}$	$P / \text{MPa}$	$v_f / \text{m/s}$		
1	3120	0.3-0.6	45.9	10.96	1.085	0.991	0.0208
2	3120	0.3-0.6	47.5	10.91	0.920	0.827	0.0175
3	3120	0.3-0.6	46.7	9.52	1.284	1.204	0.0294
4	3120	0.3-0.6	40.8	7.89	1.087	0.924	0.0341
5	2630	0.425-0.85	43.0	8.89	0.958	0.843	0.0197
6	2630	0.425-0.85	44.8	8.27	1.170	1.026	0.0135
7	2630	0.425-0.85	46.2	9.58	1.025	0.964	0.0250
8	2630	0.425-0.85	38.6	7.89	1.128	0.992	0.0303

Table 2

Velocity and displacement comparisons between measured and numerical results..

No.	Proppant condition		SC-CO <sub>2</sub> condition			Average velocity error %	Average displacement error %
	$\rho_p / \text{kg/m}^3$	$d_p / \text{mm}$	$T / ^\circ\text{C}$	$P / \text{MPa}$	$v_f / \text{m/s}$		
1	3120	0.3-0.6	45.9	10.96	1.085	8.23	1.69
2	3120	0.3-0.6	47.5	10.91	0.920	4.05	3.57
3	3120	0.3-0.6	46.7	9.52	1.284	7.40	4.80
4	3120	0.3-0.6	40.8	7.89	1.087	5.30	5.49
5	2630	0.425-0.85	43.0	8.89	0.958	4.15	4.41
6	2630	0.425-0.85	44.8	8.27	1.170	7.95	1.25
7	2630	0.425-0.85	46.2	9.58	1.025	6.35	2.96
8	2630	0.425-0.85	38.6	7.89	1.128	3.48	2.05

**Supplementary Material**

[Click here to download Supplementary Material: Supplementary---Experimental conditions in video.docx](#)

**Supplementary Material**

[Click here to download Supplementary Material: Figure 2.opj](#)

**Supplementary Material**

[Click here to download Supplementary Material: Figure 3.opj](#)

**Supplementary Material**

[Click here to download Supplementary Material: Figure 4.opj](#)



**Supplementary Material**

[Click here to download Supplementary Material: Figure 5.opj](#)

**Supplementary Material**

[Click here to download Supplementary Material: Figure 6.opj](#)

**Supplementary Material**

[Click here to download Supplementary Material: Supplementary---Lab Video.mp4](#)

**Supplementary Material**

[Click here to download Supplementary Material: Editorial Certificate.pdf](#)